Understanding Small-Molecule Interactions in Metal–Organic Frameworks: Coupling Experiment with Theory

*Jason S. Lee, Bess Vlaisavljevich, David K. Britt, Craig M. Brown, Maciej Haranczyk, Jeffrey B. Neaton, Berend Smit, Jeffrey R. Long, and Wendy L. Queen**

Metal–organic frameworks (MOFs) have gained much attention as next-generation porous media for various applications, especially gas separation/storage, and catalysis. New MOFs are regularly reported; however, to develop better materials in a timely manner for specific applications, the interactions between guest molecules and the internal surface of the framework must first be understood. A combined experimental and theoretical approach is presented, which proves essential for the elucidation of small-molecule interactions in a model MOF system known as M_2(dobdc) (dobdc^{4-} = 2,5-dioxido-1,4-benzenedicarboxylate; M = Mg, Mn, Fe, Co, Ni, Cu, or Zn), a material whose adsorption properties can be readily tuned via chemical substitution. It is additionally shown that the study of extensive families like this one can provide a platform to test the efficacy and accuracy of developing computational methodologies in slightly varying chemical environments, a task that is necessary for their evolution into viable, robust tools for screening large numbers of materials.

1. Introduction

Separation processes consume an estimated 10–15% of global energy.[1] With the expectation that this consumption will greatly increase with population growth and the implementation of large-scale carbon capture and sequestration technologies, there are intensive scientific efforts focused on the development of new physical adsorbents that might enable more energetically favorable gas separation, relative to traditional distillation or absorption processes. This feat is not easy, as the differences in the molecules of interest, such as CO_2 and N_2 – the main components in a post-combustion flue gas, are minimal.[2,3] As such, these separations require tailor-made adsorbent materials with molecule-specific chemical interactions on their internal surface.[4,5] Metal–organic frameworks (MOFs) are a particularly attractive class of porous adsorbents that are under intense investigation for gas separation due to their unmatched structural versatility. Many stable, 3D frameworks that offer unprecedented internal surface areas and the selective adsorption of a wide range of small guest molecules have been discovered.[6] The molecular nature of the organic ligand in an MOF provides a convenient modular approach to their synthesis and facile chemical tunability, creating a surge towards the directed design of new materials (**Figure 1**).[7–9] Through judicious selection of the ligand and metal, which control pore size/shape and MOF–adsorbate interactions, MOF uptake properties,

J. S. Lee, Dr. D. K. Britt, Prof. J. B. Neaton, Prof. W. L. Queen
The Molecular Foundry
Lawrence Berkeley National Laboratory
Berkeley, CA 94720, USA
E-mail: wendy.queen@epfl.ch
J. S. Lee, Dr. B. Vlaisavljevich, Prof. B. Smit
Department of Chemical and Biomolecular Engineering
University of California
Berkeley, CA 94720, USA
Dr. C. M. Brown
National Institute of Standards and Technology
Center for Neutron Research
Gaithersburg, MD 20899, USA
Dr. C. M. Brown
Department of Chemical Engineering
University of Delaware
Newark, DE 19716, USA
Dr. M. Haranczyk
Computational Research Division Lawrence
Berkeley National Laboratory
Berkeley, CA 94720, USA
Prof. J. B. Neaton
Department of Physics
University of California
Berkeley, CA 94720, USA
Prof. B. Smit, Prof. W. L. Queen
Department Institut des Sciences et Ingénierie Chimiques
Ecole Polytechnique Fédérale de Lausanne (EPFL)
CH 1015 Lausanne, Switzerland
Prof. J. R. Long
Department of Chemistry
University of California
Berkeley, CA 94720, USA
Prof. J. R. Long
Division of Materials Sciences
Lawrence Berkeley National Laboratory
Berkeley, CA 94720, USA

DOI: 10.1002/adma.201500966

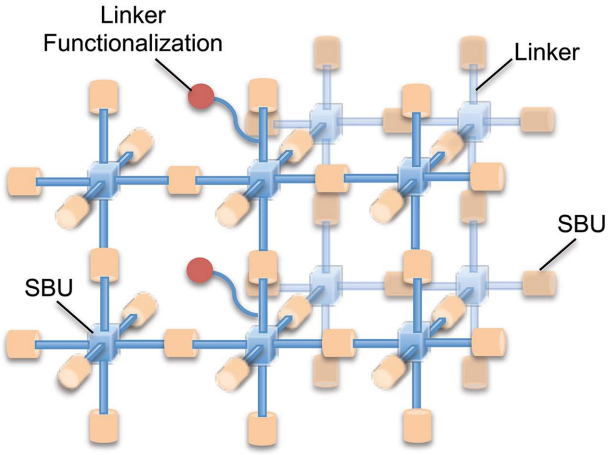

Figure 1. Cartoon image depicting the structural versatility of metal–organic frameworks (SBU = secondary building unit and represents metal-ions or metal-ion clusters).

such as gas selectivity, can be tuned.[10] While there have been many MOFs discovered to date that exemplify future promise in a myriad of applications such as gas storage[11–15] and separation,[10,16–18] catalysis,[19–21] and sensing,[22] the rate at which materials with optimal properties are discovered is still limited by empirical exploratory syntheses, which sometimes require hundreds or even thousands of chemical reactions to isolate a single, new, porous hybrid framework. As such, computational efforts, focused on both the structure and property prediction of MOFs, are currently underway.[23] The development of computational methodologies that might provide experimentalists with targeted frameworks with predefined function would significantly aid their rapid implementation for technological exploitation, a paradigm that defines research-funding initiatives such as the Materials Genome.[24]

Although the process of performing theory and simulation can be faster than its experimental counterpart, the accuracy of simulation tools will govern which types of predictions can be made and the types of systems that can be studied.[25,26] As such, experiments are often required for validation of developing computational models. This practice will allow their evolution into viable tools that can be used to answer experimentally intractable questions pertaining to structure–property relationships in large numbers of hypothetical (not yet synthesized) MOFs[27] and to evaluate the performance of reported structures for varying applications.[28] Here, we highlight the importance of coupling experimental and theoretical efforts to understand small-molecule interactions within metal–organic frameworks; while this partnership has been difficult to forge in the past, its presence is becoming more prevalent throughout the literature and will certainly have a strong impact in the implementation of MOFs in many energetically relevant applications in the future.

2. MOFs with Open Metal Coordination Sites

In many MOFs, weak van der Waals (vdW) forces are the dominant interactions between the framework and surface-bound guest species; recent work has shown that an effective strategy to increase binding energy and hence the surface packing density of adsorbates is through the generation of MOFs that contain high concentrations of coordinatively unsaturated metal centers.[29] These open metal sites are shown to induce framework selectivity in the adsorption of small molecules and provide a mechanism for charge transfer on the framework surface.[30–33] While open metal sites provide strong interactions allowing gas adsorption at higher temperatures and lower pressures than typically used for energy-consuming cryodistillation processes, the adsorbate–adsorbent interactions are often weak relative to the formation of chemical bonds, providing facile release of the molecules during the regeneration step of a separation process. Recent work by McDonald and co-workers also revealed that certain diamines, grafted to open metal sites, can offer strong, selective binding of CO_2 at low pressures (ca. 400 ppm at room temperature),[34,35] properties that are maintained even after water exposure.[36] All of these attributes have brought understanding of small-molecule interactions in materials with open metal sites to the forefront of MOF chemistry. One of the most well-studied MOFs to date is M_2(dobdc), alternatively known as M-MOF-74 or CPO-27-M, where M = Mg, Mn, Fe, Co, Ni, Cu, or Zn (**Figure 2**).[30,37–44] The significance of

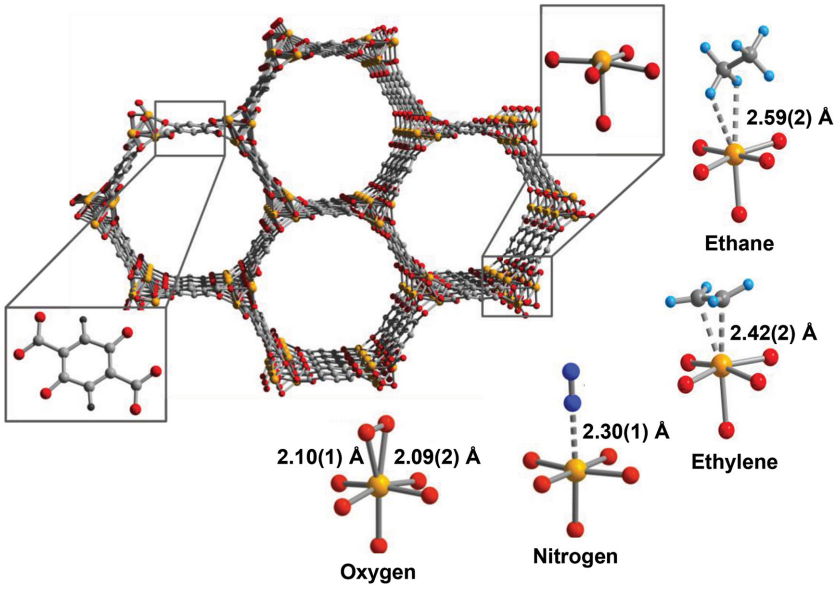

Figure 2. Ball and stick model of the Fe_2(dobdc) framework, featuring 1D honeycomb-like channels that are lined with open Fe(II) sites (top right) and 2,5-dioxido-1,4-benzenedicarboxylate ligands (bottom left). The open metal sites offer selective binding of O_2 over N_2, as well as C_2H_4 over C_2H_6; the binding mechanisms (right) were unveiled by neutron powder diffraction.[30,31] The metal, carbon, oxygen, nitrogen, and deuterium atoms are drawn as orange, grey, red, royal blue, and light blue spheres, respectively. Ball and stick model of M_2(dobdc) structure): reproduced with permission.[69] Copyright 2014, The Royal Society of Chemistry.

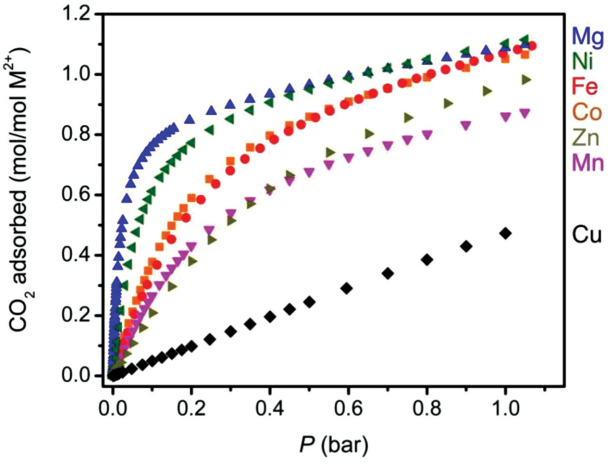

Figure 3. Excess CO_2 adsorption isotherms collected for the M_2(dobdc) series at 298 K. Reproduced with permission.[69] Copyright 2014, The Royal Society of Chemistry.

this framework is related to the interesting adsorption properties that derive from the existence of unique structural features. For instance, upon solvent removal, this material offers one of the highest densities of open metal sites of any framework discovered to date. It also undergoes chemical substitution with a wide range of first-row transition metals, which is perhaps only rivaled by MOFs of the type M-BTT (BTT^{3-} = 1,3,5-benzenetristetrazolate), where M = Mn, Fe, Co, Ni, Cu or Cd,[45–48] and M_3(btc)$_2$ (btc^{3-} = 1,3,5-benzenetricarboxylate), where M = Cr, Cu, Zn, Mo, or Ru,[49–53] providing a mechanism for tuning the adsorption properties (**Figure 3**) whilst retaining the same framework bonding motif.[54] Furthermore, all structural analogs within the M_2(dobdc) family are of high crystalline quality, allowing for detailed studies of structure–property relationships and providing an experimental platform to test how accurately developing force fields can describe the guest interaction in slightly varying chemical environments.[55,56] Recent studies on this framework encompass a wide range of experimental and theoretical methodologies utilized to characterize interactions with various guests in the M_2(dobdc) compound family (Figure 3).[57] While this is certainly not the only important MOF, it is highly prominent and has been the focus of many theoretical and experimental studies alike and consequently was chosen to be our focus within the context of this article.

3. Examples of Studies Coupling Experiment and Theory

3.1. CO_2 Adsorption in the M_2(dobdc) Series

The realization that Mg_2(dobdc) exhibits an exceptionally high CO_2 uptake at low pressure (<0.1 bar, Figure 3) and room temperature, as well as rapid, reversible adsorption/desorption of CO_2, sparked much interest in this framework for post-combustion CO_2 capture.[58,59] While it was hypothesized from high initial isosteric heats (–47 kJ mol^{-1}),[40] derived from gas-adsorption measurements, that CO_2 molecules preferentially bind at the open metal site, other methods such as diffraction, IR and Raman spectroscopy, and density functional theory (DFT) have been used to afford direct evidence of the location and orientation of CO_2 molecules binding within the pore.[60–65] From neutron powder diffraction (NPD) data, it has been found that CO_2 molecules bind in an "end-on" orientation with Mg–O(CO_2) distances and angles that range from 2.24 to 2.39 Å and 125 to 144°, respectively, depending on the CO_2 loading level.[60] These results agree well with DFT-derived Mg–O(CO_2) distances and angles computed at the B3LYP-D level to be 2.31 Å and 129°, respectively.[63]

While the local structure around the CO_2 adsorption site seems to agree well with theoretical efforts, there has been on-going debate within the MOF community as to whether the CO_2 molecule adsorbs in a linear or non-linear geometry. This debate is an important one, as intramolecular bending has strong implications for proposals that have been made to utilize MOFs with open metal sites for the activation and chemical conversion of CO_2. Several diffraction studies show that the O–C–O angle within the adsorbed CO_2 molecule deviates significantly, >15°, from the expected 180°;[60,66] however, first-principles studies carried out by Wu et al. indicate a significant energy penalty for such a bend;[64] this result calls into question whether the experimentally determined bending could be the result of a misinterpretation of the diffraction data due to statically disordered molecules on the framework surface. This debate has since been laid to rest as a recent study shows that an improvement in the crystalline quality of Mg_2(dobdc) and slowly cooling the CO_2-adsorbed sample before the diffraction experiments yields an intramolecular CO_2 angle with minimal deviation from the expected linear geometry, 179(2)°. Within the error of the experiment, bending cannot be observed. While this work shows a nice correlation between experiment and theory, it also highlights the importance of sample quality and proper handling.

While many of the aforementioned techniques have indicated that the exposed open metal sites are the preferential binding sites for CO_2 in Mg_2(dobdc), a gap in understanding the diffusive properties of CO_2 is still elusive. ^{13}C NMR measurements of CO_2 adsorbed Mg_2(dobdc)[67] have been carried out, revealing a distinct chemical shift anisotropy (CSA) powder pattern, which was, at the time, interpreted to be the result of a uniaxial rotation with a fixed rotation angle θ that ranged from 56° to 69° (200 K to 400 K). However, a more recent study used molecular simulations to probe the free-energy landscape of CO_2 in Mg_2(dobdc) under conditions similar to those used in the NMR study. Monte Carlo simulations, used to simulate CSA powder patterns, suggested that the NMR signature was instead the result of a molecular-hopping motion between metals within the crystallographic *ab* plane, indicating that the dynamics of CO_2 within Mg_2(dobdc) were likely more complex than originally expected (**Figure 4**).[68]

Since these studies of CO_2 adsorption in Mg_2(dobdc), several combined experimental and theoretical approaches have been taken to identify the host–guest interactions that lead to significant differences in isosteric heats among all of the metal-substituted analogs in the M_2(dobdc) series.[54,69] Among those members, isosteric heats of adsorption (Figure 3) follow a trend (Mg > Ni > Co > Fe > Mn > Zn >Cu) that unexpectedly does not correlate with the ionic radii.[68] A recent study by Yu

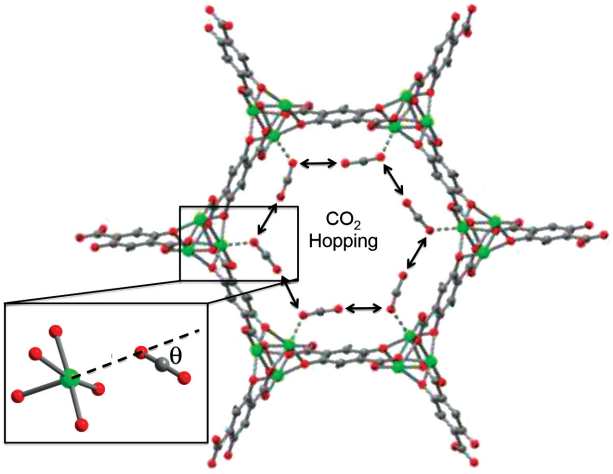

Figure 4. Ball and stick model of Mg_2(dobdc) with CO_2 adsorbed at the open metal site, as determined by NPD. The arrows represent the CO_2-hopping mechanism proposed by molecular simulations used to interpret NMR data. The higher-magnification view represents the fixed rotation angle, θ. The green, red, and grey spheres represent Mg, O, and C, respectively.

et al.[54] gives an explanation for the observed trend through a description of nuclear screening effects by M^{2+} d-orbitals. Their first-principles study reveals that the relative strength of the electrostatic interaction is dictated by the effective charge of the metal cation at the open coordination site where the CO_2 binds. The most recent study of CO_2 adsorption in M_2(dobdc) additionally used diffraction experiments to unveil the site-specific binding properties of CO_2 within most of the analogs. DFT calculations accounting for vdW interactions quantitatively corroborate and rationalize the observations regarding intramolecular CO_2 angles and trends in relative geometric properties and heats of adsorption in the M_2(dobdc)–CO_2 adducts (**Table 1**). Huck et al.[70] compared the different metals in their performance for carbon capture and showed that for an ideal dry flue-gas mixture, the Mg version of M_2(dobdc) performed optimally. However, Lin and co-workers[56] showed that the presence of a trace amount of water makes Mg_2(dobdc) lose its selectivity.[68]

Of particular interest was the weakest CO_2 adsorbent, Cu_2(dobdc) (Figure 3). The structural analysis of this framework resulted in a local minimum with CO_2 bound in a parallel orientation with the framework wall, rather than bound to the open metal site, a result that did not agree with the vdW-DF2 calculations. To investigate this mismatch between experiment and theory, the nudged elastic band transition state method,[71] was used to assess the potential existence of a kinetic barrier between the two structures. When no such barrier was found, high-intensity diffraction data obtained from a synchrotron source was assessed. The data revealed a secondary adsorption site unidentified in the lower-intensity NPD data, a direct result of weakly bound/slightly disordered CO_2. Assignment of the secondary site resulted in stabilization of the expected structural model proposed from DFT, with CO_2 adsorbed at the open metal, and an overall improvement in the structural refinement.[69]

Given the recent success of computational methods in the prediction of adsorbate interactions with open metal sites, as determined through experimental validation, recent quantum mechanical calculations have been applied to predicting the CO_2 adsorption properties of hypothetical materials within the M_2(dobdc) family. The goal is to provide experimentalists with guidance toward synthesizing the most-useful materials. A recent study of Poloni et al.[72] utilized vdW-corrected DFT and a local chemical bond analysis to explain trends in the binding between CO_2 and open metal sites. They, and others[73] suggest that two yet-to-be synthesized materials, V_2(dobdc) and Ti_2(dobdc), would exhibit CO_2 binding energies that are significantly stronger than any of the existing analogs. They reason their result using the electronic configuration of these two divalent cations and symmetry of the metal coordination site upon CO_2 binding, which give rise to empty antibonding orbitals between the CO_2 and the metal cation. It is additionally worth noting that other studies have predicted, using both DFT and quantum-chemical methods, that V_2(dobdc) could be of potential utility for the separation of N_2 from CH_4, a particularly challenging separation, which is of critical value in natural-gas utilization.[74] The vanadium(II) ions have a binding energy that is significantly increased due to π back-bonding with N_2 but not with CH_4. While both these theoretical efforts give a target

Table 1. Experimental and theoretical (DFT) data, comparing CO_2 adsorption properties of the M_2(dobdc) series.[a)]

M	M···O(CO_2) [Å]		∠ O–C–O(CO_2) [°]		∠ M–O–C(CO_2) [°]		$-Q_{st}$[b)] [kJ mol^{-1}]	$-\Delta H$[c)] [kJ mol^{-1}]
	Experiment	Theory	Experiment	Theory	Experiment	Theory	Experiment	Theory
Mg	2.27(1)	2.41	178(2)	178.3	131(1)	123.8	43.5(2)	40.9
Mn	2.51(3)	2.57	176(3)	178.8	120(2)	122.2	31.7(1)	33.9
Fe	2.29(3)	2.62	179(3)	178.7	106(2)	120.6	33.2(1)	34.1
Co	2.23(4)	2.56	174(4)	178.7	118(2)	118.6	33.6(1)	33.8
Ni	2.29(3)[d)]	2.52	162(3)[d)]	178.6	117(2)[d)]	120.1	38.6(6)	37.3
Cu	2.86(3)	2.87	180(2)	179.1	117(1)	112.4	22.1(2)	27.1
Zn	2.43(4)	2.84	178(6)	178.7	117(3)	114.6	26.8(1)	30.2

[a)]Values reported are from ref. [69] unless otherwise specified; structural parameters from NPD data were obtained from CO_2 loadings ranging from 0.35 to 0.82 CO_2 per M^{2+} at 10 K; [b)]Low-coverage CO_2 isosteric heats of adsorption for the M_2(dobdc) analogues were calculated at a loading of 0.1 CO_2 per M^{2+}; [c)]Theoretical values were calculated using 0 K DFT binding enthalpies corrected at the harmonic level for ZPE and TE contributions, at loadings of 0.167 CO_2 per M^{2+}. The DFT binding energies on which these binding enthalpy calculations are based were published in ref. [72]; [d)]Values were reported by Dietzel et al. in ref. [39].

for experimentalists to synthesize, to date the reaction conditions necessary for the isolation of V_2(dobdc) or Ti_2(dobdc) have not been identified. This lack of success calls into question the experimental feasibility of theoretical targets. As such, computational methods to help identify the practicality of materials synthesis through predictions of potential reaction conditions will be a worthwhile effort in the future.

Aside from structural properties, a strong synergy between experiment and theory exists in the prediction of adsorption isotherms. The exceptional capacity for CO_2 adsorption in Mg_2(dobdc) cannot be reproduced with off-the-shelf force fields, as they do not properly describe the CO_2–metal interaction. However, quantum-chemical methods can be used to fit force fields from ab initio. Dzubak et al.[75] showed that by fitting a force field from the interaction energies of a cluster model of Mg_2(dobdc) at the MP2 level of theory, adsorption isotherms can be computed in good agreement with experimental data. Furthermore, by comparing the computed and experimentally determined isosteric heats of adsorption, they showed that approximately 20% of the metal sites are not accessible in the experimental structure. This finding was recently supported by an experimental study, which revealed, from a combination of diffraction data and adsorption measurements, that a large percentage of open metal sites in the M_2(dobdc) series, up to 30%, are inaccessible.[69] Subsequently, Lin et al.[56] developed a scheme to fit force fields from periodic DFT (vdW-DF2 in particular) eliminating the need to choose a cluster model. In this work, CO_2 and water force fields were developed and, by calculating mixture isotherms, they discovered that CO_2 uptake drops to nearly zero even when small amounts of water are present. Studies like these are successful if one wishes to study a particular framework for which force fields in the literature fail; however, challenges remain when MOFs with open metal sites are included in screening studies of large databases. Ongoing work in this area focuses on first identifying materials with open metal sites, computing charges for a large database, and improving the force fields used in screening to reliably capture binding at the open metal site.

3.2. Hydrocarbon Separation in M_2(dobdc)

Likewise, members of the M_2(dobdc) family have shown significant promise for the separation of light hydrocarbons, namely paraffin/olefin mixtures such as ethane/ethylene and propane/propylene.[31,76] These separations, which are currently carried out via distillation at low temperatures and high pressures, are among the most energy consuming in the chemical industry.[77] A physical adsorbent that could permit an efficient paraffin/olefin separation at higher temperatures could offer remarkable energy savings.

An in situ diffraction study revealed that the high selectivity of O_2 over N_2 observed in Fe_2(dobdc) resulted from π-complexation of the open iron(II) site with oxygen, as indicated by a side-on binding mechanism (Figure 2);[30] this discovery led Bloch et al.[31] to subsequently begin investigating olefin/paraffin separations in this same analog. Single-component isotherms, breakthrough experiments, and NPD were used to determine isosteric heats and selectivities, the separation ability of binary mixtures, and the binding geometries of C2 and C3 hydrocarbons, respectively. Results from the single-component isotherms indicated a high affinity for unsaturated hydrocarbons versus their saturated counterparts, and NPD also revealed the expected side-on binding for acetylene, ethylene, and propylene (Figure 2). Breakthrough experiments, carried out on equimolar mixtures of ethane/ethylene and propane/propylene at 318 K, indeed revealed good separation performance, with greater than 99% purity (at 318 K) of the separated components in all cases.[31]

As breakthrough experiments are extremely time consuming, Krishna and co-workers,[31,76] in parallel, developed methodologies to simulate the breakthrough characteristics to assess many materials and for a variety of industrially relevant hydrocarbon separations. The aforementioned experimental results were first used to validate these tools to show that the simulations could reproduce breakthrough experiments obtained from Fe_2(dobdc) with reasonable accuracy. Then, the tools were subsequently applied to make quantitative comparisons with many other competitive adsorbent materials, including both zeolites and other MOFs with open metal sites; the studies indicate the superiority of Fe_2(dobdc) for paraffin/olefin separations over all of those computationally analyzed. These predictive tools were additionally applied to simulate breakthrough experiments for the iron(II) analog in a quaternary gas mixture including methane, ethane, ethylene, and acetylene at 318 K. While this separation is of high importance in the purification of natural gas, breakthrough experiments with such complex gas mixtures are still experimentally intractable. The simulation results suggest a successful separation could be carried out (**Figure 5**) with three adsorbent beds packed with Fe_2(dobdc). Finally, the tools were used to assess the separation of low concentrations of acetylene (0.01 bar) from ethylene (1 bar), as the former is not tolerable in ethylene-polymerization reactors. The simulations suggest that acetylene concentrations of approximately 10 ppm could be realized at 318 K with Fe_2(dobdc) as

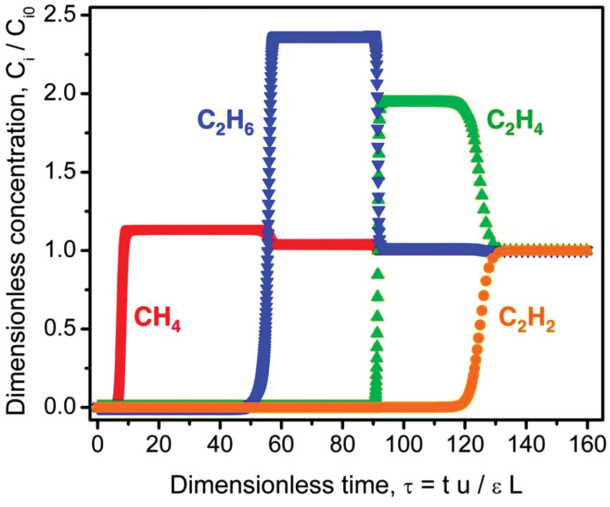

Figure 5. Simulated breakthrough curves for an equimolar mixture of methane, ethane, ethylene, and acetylene at 1 bar flowing through a bed of Fe_2(dobdc) 318 K. Reproduced with permission.[31] Copyright 2012, American Association for the Advancement of Science.

the solid adsorbent.[31] All of these studies are prime examples that highlight the evolution of computational tools and their application in assessing materials properties that would otherwise be experimentally challenging.

Since then, several other comprehensive experimental and theoretical studies have been carried out to assess other metal-substituted analogs of M_2(dobdc).[65,76,78,79] Geier et al.[79] demonstrated from adsorption-isotherm data and breakthrough experiments collected on the Mg-, Mn-, Fe-, Co-, Ni-, and Zn-containing analogs that the highest achievable separation selectivity for ethane/ethylene and propane/propylene could be realized with the Fe^{2+} and Mn^{2+} analogs, respectively (from 318 to 358 K). In a recent study, Lee et al.[65] utilized vdW-DF2 with Hubbard *U* corrections to assess 140 unique systems; they studied 10 metal-substituted M_2(dobdc) analogs, both hypothetical and known, and their interactions with 14 different small molecules, including C1–C3 hydrocarbons. Compared with experimental results, the theoretically predicted binding geometries and enthalpies indicated good agreement across all the hydrocarbon systems studied, with the exception of C_3H_8, which has more internal degrees of freedom relative to other small molecules, making it difficult to resolve the global minimum.

To the best of our knowledge, only a few other theoretical studies have been applied to understand small-hydrocarbon–M_2(dobdc) interactions, and those are solely focused on the Fe^{2+} analog. Verma et al.[80] studied an 88-atom (3 Fe atoms) and a 106-atom (5 Fe atoms) cluster model using the M06L functional for C1–C3 hydrocarbons. While they were able to show that unsaturated hydrocarbons adsorb more strongly to open metal sites than saturated analogs and accurately predict the trend observed in the experimentally determined binding enthalpies ($C_2H_2 > C_2H_4 > C_3H_6 > C_3H_8 > C_2H_6 > CH_4$), the calculated enthalpies overestimated the experimental values by 8.4 to 20.9 kJ mol^{-1}. Furthermore, the binding energy was decomposed and the damped dispersion term was shown to correlate with the bonding trends observed, with the exception of acetylene. Additionally, Kim et al.[81] used first-principles calculations to determine the orbital interactions between the open metal site and C1–C3 hydrocarbons, allowing them to directly assess the olefin/paraffin separation ability in Fe_2(dobdc). Their periodic DFT calculations were equipped to fully describe both intermolecular interactions and magnetic ordering from the host lattice. They found that the highest occupied molecular orbital (HOMO) of the paraffin only weakly interacts with iron(II) without back-donation, implying that the separation is predominately facilitated by the well-known π-interaction of the olefins. However, intermolecular interactions and magnetic ordering of the host lattice have also shown to make a significant contribution to the binding energy, 2–28% and 6–8% respectively.[81]

It is clear from the aforementioned results that many computational methodologies have been used to assess hydrocarbon interactions in this extensive family of MOFs; however, it is worth noting that the comprehensive experimental study presented by Geier et al.[79] also shows that methods of sample preparation and activation greatly influence materials performance. As such, we again reiterate that experimental efforts focused on maximizing the sample quality are an essential component when trying to draw direct correlations between experimental and theoretical results.

3.3. Small-Molecule Activation and Conversion in M_2(dobdc)

While most of this article has focused on gas separation, which is reliant on weaker, electrostatic-type interactions between open metal sites and adsorbates, open metal coordination sites also offer an opportunity for charge transfer on the pore surface, making the line between gas separation and chemical conversion on some occasions a bit obscure. This was highlighted in a recent study of O_2/N_2 adsorption in Fe_2(dobdc).[30] While it was determined that the material was highly selective for O_2 over N_2, it undergoes a crossover from a physisorption to a chemisorption regime (above 225 K), rendering the O_2 adsorption process irreversible. It was found that the framework undergoes oxidation to form Fe^{3+} and a surface-bound peroxide species, as determined by a significant elongation in the O–O distance from 1.25(1) to 1.6(1) Å.[30] Maximoff and Smit[82] explained these observations in terms of charge-transfer-mediated adsorption of electron-acceptor oxygen molecules in the MOF, which is driven by quasi-1D metal–insulator–metal transitions that localize or delocalize the quasi-1D electrons.

This study and many others[32,83–88] have bolstered interest in developing new MOF platforms that offer catalytically active sites for the conversion of small molecules into value-added chemicals, a task that offers a strong economic and environmental payoff. MOFs offer many attractive features as heterogeneous catalysts, which include well-defined and isolated active sites that potentially prevent unwanted side reactions, crystalline lattices that are conducive to understanding structure–property relationships, and size, shape, and chemical exclusion that can make reactivity and product formation selective. One recent example in the literature shows a comparative study between Mg_2(dobdc) and Ni_2(dobdc) for the gas-phase oligomerization of propylene into longer-chain hydrocarbons (at 453 K and 5 bar), a study relevant to the production of liquid fuels and detergents. While the Mg^{2+} analog was found to be inactive, the Ni^{2+} derivative showed not only a relatively good reactivity compared with Ni^{2+}-exchanged aluminosilicates but also a significantly higher selectivity for the production of linear over branched chain oligomers. The increase in selectivity is likely related to steric effects that result from active Ni^{2+} sites embedded in the MOF wall.[88]

While it is possible, in principle, to rationally design the active site and control its surrounding environment with an unparalleled degree of precision, MOFs also have several limitations related to their stability and, as a result, long term cyclability.[89] With few tandem experimental and theoretical studies, there is currently a lot of room for strong partnerships, particularly related to targeted design of materials with predefined function, identifying reaction mechanisms or short-lived reaction intermediates, and understanding mechanical, chemical, and thermal stability of materials in various application relevant environments. While it is not our goal to review heterogeneous catalysis in MOFs, as that has been done elsewhere,[90–93] we will briefly highlight a couple of tandem studies involving M_2(dobdc).

Efficient catalysts that can aid in the activation C–H bonds could help to transform the chemical industry by allowing the conversion of cheap, abundant alkanes into other valuable organic compounds. Currently, activation is readily carried out in nature by metalloenzymes, but mimicking this reactivity is quite

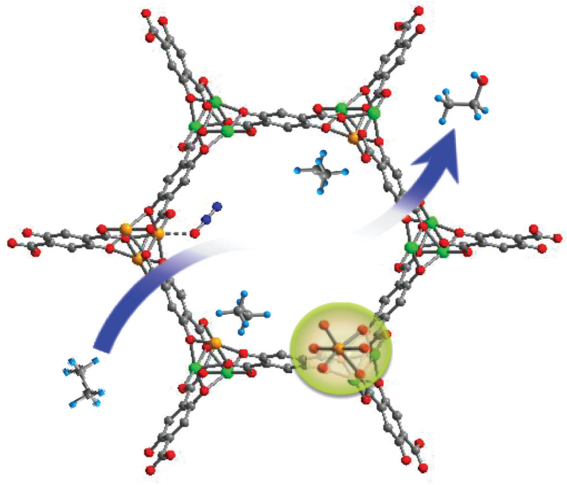

Figure 6. Ball and stick model of $Fe_{0.1}Mg_{1.9}(dobdc)$[94] showing ethane conversion to ethanol after framework oxidation with N_2O, which likely forms a transient Fe(IV)-oxo. The green, orange, grey, red, dark blue, and light blue spheres are Mg, Fe, C, O, N, and D, respectively.

difficult in synthetic systems that do not have the protective protein superstructure, making reactive iron(IV)–oxo sites susceptible to decomposition. A recent study by Xiao et al.[94] showed the conversion of ethane to ethanol with N_2O oxidation of $Fe_2(dobdc)$ (**Figure 6**). NPD was first used to unveil the binding mechanism of N_2O at low temperatures where the coordination is reversible. It revealed the Fe^{2+}–N_2O adduct has mixed η^1-O and η^1-N coordination, with distances of 2.42(3) Å and 2.39(3) Å from the metal, respectively. This was further validated by DFT studies with the M06 functional, which also showed that η^1-O is favored over η^1-N by only 1.1 kJ mol^{-1}, further supporting the observation of mixed coordination. When heating the N_2O-dosed framework to 348 K, there is an irreversible transformation to $Fe_2(OH)_2(dobdc)$ with an Fe–OH distance of 1.91(1) Å, a value that was further corroborated both by extended X-ray absorption fine structure (EXAFS) measurements and periodic DFT calculations. When the framework is heated in mixtures of N_2O, Ar, and ethane, the reaction yields various ethane-derived products. The authors proposed that a short-lived iron(IV)–oxo is the active species; however, they were unable to capture this using these standard characterization methods as it quickly decomposes to an iron(III)-containing material, $Fe_2(OH)_2(dobdc)$. Electronic-structure calculations via periodic DFT (PBE+*U*) and a cluster model at the M06/M06L level of theory were used to characterize the active site. Both methods predict the existence of a quintet ground state with a short Fe–O bond distance of 1.64 Å, a value consistent with previously characterized iron(IV)–oxo species.[94] It should be additionally noted that the authors synthesized a material that was diluted with Fe^{2+}, $Fe_{0.1}Mg_{1.9}(dobdc)$, in the hope of separating the reactive sites and inhibiting other side reactions. Indeed, this yielded the exclusive formation of ethanol and acetaldehyde (in a 10:1 ratio).

To the best of our knowledge, other combined theoretical and experimental studies focused on small-molecule activation and conversion in the $M_2(dobdc)$ compounds appear to be limited to a recent study of Tan et al.[95] that investigates the water dissociation mechanism on the surface of several $M_2(dobdc)$ analogs. This understanding is very difficult in many materials, such as nanocrystals, that rely on surface defects as active sites, making the process much less straightforward to characterize; however, MOFs, particularly the system of interest, offer a nice means to study water dissociation on open metal sites with easy structural characterization. In this study, the authors used a combination of in situ IR spectroscopy with first-principles calculations to characterize the materials. They found a dissociation of D_2O at temperatures above 423 K, as determined by the appearance of an absorption band at 970 cm^{-1}. DFT calculations indicate the O–D bend is attributed to that of a D atom attached to the phenolate linker, while the $(OD)^-$ binds to the metal. It was suggested that the reactivity of the metal-substituted frameworks has the following trend: Zn> Mg > Ni > Co, as determined by the intensity of the absorption bands for each material under the same conditions; however, the authors make no assessment of sample quality nor the number of open metal sites likely available in the materials, which has proven important in many previous studies.[69]

4. Characterization of MOFs

4.1. Experimental Approaches, Limitations, and the Need for Theory

Since the discovery of the first MOF with open metal sites, Zn(bdc) (bdc = 1,4 benzenedicarboxylate),[96] synthetic efforts based on multiple strategies have led to the generation of many materials that contain open metal sites. These approaches include the incorporation of metalloligands[97–99] and syntheses where metal clusters containing open metal sites are used ab initio.[100,101] In other cases, serendipity has led to the incorporation of solvent into a coordination site of the metal, upon framework formation.[49] In any of these instances, activation procedures, which are typically carried out with a combination of vacuum and heat, are necessary to liberate solvent molecules from the metals for subsequent in situ characterization of adsorption properties.

For most in situ measurements, customized cells are integrated with gas-dosing manifolds that deliver predefined amounts of adsorbate to materials that are then cooled or heated in situ to the temperature regime of interest. For example, for measurements meant to unveil static structural properties, low temperatures less than 100 K are typically used, while for spectroscopic measurements, used to observe phenomena such as diffusion, much higher temperatures are often required to activate dynamic modes.[67] Much recent effort has also been put into studying materials in more-application-relevant environments, such as high pressures and temperatures that are required for many gas-storage and separation applications; these studies are focused on unveiling information related to framework flexibility and mechanical stability.[102]

With most practical applications of MOFs reliant on specific interactions with small guest molecules, understanding these interactions is a necessity to interpret the properties of existing frameworks, and in turn, inform the design of new and improved MOFs with desired function. The crystalline nature of these materials gives rise to a non-homogeneous potential-energy landscape that dictates how incoming guest species arrange

themselves on the framework surface. As such, in situ diffraction techniques are the most-direct way to characterize static host–guest interactions, and are particularly powerful when paired with adsorption measurements. Diffraction can reveal, for example, the location and orientation of static guest molecules, relative differences in binding energies between sites, the nature of binding interactions, and the framework response to various stimuli, such as pressure and temperature.

While in situ structural characterization of MOFs has become relatively common, there are inherent limitations in this approach. For instance, position- and time-averaged diffraction experiments can be limited by static or dynamic disorder, making it difficult to elucidate, on some occasions, the fine structural detail associated with important bond angles and distances. These problems can become even more significant with variations in sample handling and low crystalline quality, as previously discussed. Recent theoretical work suggests that inconsistencies of the crystal-structure inputs obtained from experimentally determined diffraction data can greatly influence the results of molecular simulation studies;[28] Dzubak et al.[75] report Grand Canonical Monte Carlo (GCMC) simulations of CO_2 adsorption isotherms from several experimentally determined structures of M_2(dobdc). It was found that the predicted adsorption isotherms obtained from the experimental data deviated greatly from the experimental isotherm, while those obtained from the DFT-optimized structures showed good agreement.[75] It was hypothesized that the lack of agreement was the result of variations in the lattice parameters from the as-prepared samples, highlighting the sensitivity of these calculations to atomic structure.[75,103]

A wide range of in situ spectroscopic methodologies such as IR and Raman,[104,105] inelastic neutron scattering (INS),[106] NMR,[67] and others[107–109] are highly sensitive to molecular interactions in porous media, and they have been used to successfully characterize various guest–framework interactions. While many of these techniques directly probe small-molecule dynamics related to rotations, vibrations, and diffusion, the resulting spectra can also be used to extract binding configurations, binding enthalpies, and even loading levels. While we do not intend to review all of these techniques individually, as they have been thoroughly covered elsewhere,[104,109–113] we would like to point out that there are limitations related to data interpretation that can be significantly aided by theoretical investigations.[114]

Information pertaining to small-molecule interactions is often extracted from line shifts, widths, and/ or intensities. There are false assumptions throughout the literature that correlate line shifts in IR, Raman, and INS spectra with adsorption energy; this is often not the case as peak positions are extremely sensitive to the coordination environment around the open metal site.[104,106,115] In addition, integrated peak intensities are often assumed to be associated with the loading level;[114] however, in systems where increased loading results in additional intermolecular interactions, this correlation does not always hold true. This was highlighted by a combined experimental and theoretical study of Nijem et al.,[116] who studied H_2 adsorption in the M_2(dbodc) series. They found that high H_2 loadings in Mg_2(dobdc) resulted in a counterintuitive decrease in IR intensity due to a decrease in the effective charge of H_2 at the open metal site. While these tools are widely accepted as a means to assess host–guest interactions, interpretation of the data should proceed with caution and, when relevant, theory that is capable of incorporating vdW interactions should be used as a tool to help interpret the data.

In many instances, computational tools have proven necessary for the interpretation of spectra. This was highlighted by the work of Lin et al.[68] wherein molecular simulations were used for the first time to reproduce CSA powder patterns of ^{13}C NMR, work that was proven to be essential for the interpretation of diffusive motions of CO_2 in Mg_2(dobdc). More recently, near edge X-ray absorption fine structure (NEXAFS), an element-specific technique, was used to probe the Mg K-edge in the activated Mg_2(dobdc), and then with DMF and CO_2, bound to the open metal site. Spectra, simulated using a DFT-based protocol and compared with the experimental spectra, proved essential in understanding the variations in the local electronic environment around the open metal site with adsorption.[107]

4.2. Computational Approaches, Limitations, and Comparison with Experiment

In the study of the adsorption properties of MOFs, there are many opportunities to draw comparisons between experiment and theory. DFT can be used to optimize structures, predict binding energies, and compute spectroscopic properties comparable with diffraction data, isosteric heats derived from adsorption measurements, and experimental spectra. On the other hand, molecular simulations such as Grand Canonical Monte Carlo (GCMC) are used to simulate single- or mixed-component adsorption isotherms, the Henry coefficient, and the heat of adsorption, while molecular-dynamics simulations are used to obtain diffusion coefficients (**Figure 7**). The development of a computational toolbox for characterization is not

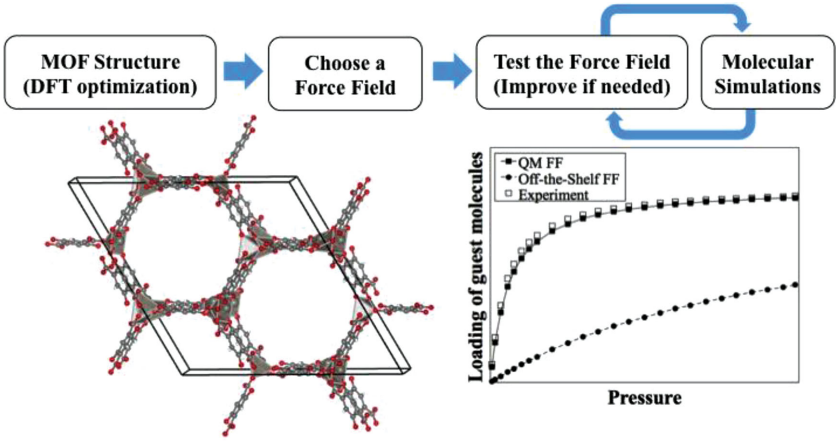

Figure 7. Steps required to obtain a reliable calculated adsorption isotherm: i) determine structure of the activated MOF; ii) choose the guest geometry and force field (e.g., all atom or united atom force field); iii) test the force-field performance and determine if any corrections or development are needed; iv) perform molecular simulation.

only meant to aid in small-scale experimental endeavors like understanding host–guest interactions in families of MOFs as presented here, but is also ultimately meant to be applied to large-scale computational screening of databases derived from both experimental and hypothetical materials. From an experimental perspective, while the synthesis of large numbers of frameworks in a high-throughput manner is already time intensive, large-scale experimental screening of materials properties is still non-existent.

For any calculation, computationally ready structure files, either derived from diffraction data or structure simulations, are first required. It should be noted that experimentally determined structures must first be corrected, so they are devoid of missing protons, adjusted for solvent, or partially occupied or disordered atoms. With this purpose in mind, the Computationally Ready, Experimental (CoRE) MOF database, which contains ca. 5000 structures that have been deemed "computationally ready" was created.[28] A hypothetical framework can also be generated either by modifying an existing experimental structure (e.g., ligand functionalization or metal substitution) or through the use of an MOF-building algorithm.[117,118] Generally, both experimental structures and those generated via assembling building blocks should be optimized by either molecular mechanics or electronic-structure calculations prior to their use. Due to the large size of the unit cells of MOFs, DFT seems to be the only viable quantum-mechanical (QM) method to study MOFs across their diverse chemistries. While the accuracy of DFT always depends on the functional, the generalized gradient approximations (GGAs) are typically in good agreement with experiment. For example, the M_2(dobdc) series (M = Mg, Mn, Fe, Co, Ni, Cu, and Zn) optimized with PBE+*U* resulted in mean absolute errors (MAEs) in the metal–oxygen bonds ranging from 0.9–2.1% and lattice constants in good agreement with experiment.[65] Finally, we should note that the current efforts in generating hypothetical structures have many limitations. For example, trade-offs in computational costs between evaluating structures for synthetic accessibility and exploring additional degrees of structural freedom make it difficult to develop a high-throughput algorithm that still yields an accurate, yet exhaustive list of predicted structures.[119]

A significant challenge in DFT is related to the development of functionals that are able to account for the contribution that dispersion forces have on adsorbate–adsorbent interactions.[120,121] The local density approximation (LDA) or GGA exchange correlation functionals do not accurately account for dispersion forces, causing an overestimation or underestimation of the interaction energies, respectively. As such, several approaches have been taken to include dispersion within the DFT formalism, including the semi-empirical correction approaches developed by Grimme (DFT-D2 or DFT-D3)[122,123] and the nonlocal vdW-DF functionals.[124,125] The vdW-DF2[124] functional, among the best-performing vdW-DF functionals, slightly overestimates distances between adsorbed guest species and the metal site; however, the binding energies are generally in good agreement with experiment. More-extravagant methods include several high-level corrections to the DFT energies, but these methods require system-specific correction factors and are not transferable from one MOF system to another. Additionally, meta-GGAs like the Minnesota functionals[126] have been shown to account for dispersion to some extent (see a recent review on vdW forces in DFT[127]). Furthermore, MOFs that contain metals with unpaired d electrons located on the metal center require the use of Hubbard *U* corrections to properly describe the electronic structure when employing periodic DFT and a plane-wave basis.[128] In open metal sites, this correction is required to properly predict the spin ground state and improve the energetics of the d band. If either is not correct, the interaction with the open metal site and the guest will not be accurate. While these QM methods have not been used in a truly high-throughput manner for screening materials, they have been applied to families of materials to understand, for example, how metal substitution affects adsorption properties.[65]

For molecular simulations, a classical force field that properly describes the host–guest and guest–guest interactions must be chosen. For other classes of porous materials (e.g., zeolites and the isoreticular MOF series), well-established force fields in the literature have been shown to perform well. However, for the strong interactions in MOFs with open metal sites, off-the-shelf force fields fail to describe the guest–open metal site interactions, underestimate the binding strength, and result in an adsorption isotherm that is in poor agreement with the experiment (Figure 7).[75,129] Two approaches have been used to develop force fields for open metal site MOFs. One approach is to employ a standard force field but scale the partial charges or empirically refit the vdW parameters in order to obtain good agreement with a set of experimental data.[130] However, this approach requires accurate experimental data and, while the adsorption isotherm or heat of adsorption may be well reproduced, it does not guarantee that the physics of the system are properly described. In other cases, force fields are fit to quantum-chemical calculations.[26,75,131–136] This approach does not require any input from experiment, but does require a significant amount of work. The choice of the level of theory for the QM calculation, to use a cluster model or periodic approach, the charge model, and the functional form of the force field are all essential choices one must make (see recent review by Yang et al.[137] for more details).

GCMC simulations have been used successfully not only to study specific MOFs, but also to perform high-throughput screening[137] of MOF databases (see recent reviews).[25] MOFs with open metal sites are particularly challenging for these types of studies. Not only is it challenging to identify which of the MOFs in the database contain open metal sites without visually inspecting each MOF, one must decide if the force field being used in the screening is able to treat that metal site appropriately. Due to the large number of MOFs included in a screening study, a new force field cannot be developed for each material, and ongoing work in this field is focused on these types of problems.

5. Future Outlook

Though progress has been made in cooperative advancement of both theory and experiment in understanding MOF–small-molecule interactions, the rate at which materials are symbiotically being discovered, characterized, and actively utilized

remains slow. One challenge is the difficulty of developing synthetic pathways toward a specific structure containing the desired building blocks. Even when a new MOF is successfully synthesized, there are few guarantees, aside from chemical intuition and empirical trends, that it can be used for the application motivating its development. Hence, a genomic approach to MOF design[23,24] would enable scientists to screen many hypothetical structures, identify those with the highest potential for a specific application, and propose possible synthetic conditions to expedite the discovery process. Alongside the computational frameworks utilizing high-level theory, computational tools, such as Zeo++,[138] are being developed to further bridge the gap between theoretical prediction and experimental synthesis, by integrating high-throughput exploration of materials space. Some of the challenges to be addressed in the near future are better control of the diversity and biases in the libraries being generated, and better assessment of synthetic feasibility during the enumeration process. Such algorithms have been published for zeolites,[139,140] and similar tools need to be developed to capture the structure and pore diversity of MOFs. Similarly, data mining and machine-learning approaches[141,142] will require more MOF-focused classifiers, including structure and pore geometry, to correlate available simulation and experimental data with possible applications. Hence, tools that do not utilize intensive QM calculations are offering valuable information, even if it's just pore geometry and species-specific accessible void space, toward guiding the discovery and application of MOFs.

These tools, along with high throughput screening with QM and GCMC methods, will push past the era of largely serendipitous MOF discoveries[143] and allow for engineered porous media for solving specific problems. Despite the successes that have been demonstrated in M_2(dobdc), transferring that success to other materials of interest and executing the "genomic approach" remains challenging. Computational tools are still uncertain as to the limits of valid MOF structures. Regardless, the MOF field continues to be a rapidly growing field for both experimental and theoretical work due to the cooperative efforts that push both to grow together.

Acknowledgements

The authors would like to acknowledge the Nanoporous Materials Genome Center of the US Department of Energy, Office of Basic Energy Sciences, Division of Chemical Sciences, Geosciences and Biosciences under Award Number DE-FG02–12ER16362 for the support of J.S.L. and W.Q. The authors would also like to acknowledge the Center for Gas Separations Relevant to Clean Energy Technologies, an Energy Frontier Research Center funded by the U.S. Department of Energy, Office of Science, Office of Basic Energy Sciences under award DE-SC0001015 for the support of C.B., J.N., B.S., and J.R.L. M.H. was supported by the Center for Applied Mathematics for Energy Research Applications (CAMERA), funded by the U.S. Department of Energy under Contract No. DE-AC02- 05CH11231.

Received: February 25, 2015
Revised: April 29, 2015
Published online: May 28, 2015

[1] J. R. Long, Center for Gas Separations Relevant to Clean Energy Technologies a DoE Energy Frontier Research Center, http://www.cchem.berkeley.edu/co2efrc/, accessed: January **2015**.
[2] D. M. D'Alessandro, B. Smit, J. R. Long, *Angew. Chem. Int. Ed.* **2010**, *49*, 6058.
[3] K. Sumida, D. L. Rogow, J. A. Mason, T. M. McDonald, E. D. Bloch, Z. R. Herm, T.-H. Bae, J. R. Long, *Chem. Rev.* **2011**, *112*, 724.
[4] J.-R. Li, J. Yu, W. Lu, L.-B. Sun, J. Sculley, P. B. Balbuena, H.-C. Zhou, *Nat. Commun.* **2013**, *4*, 1538.
[5] J.-R. Li, Y. Ma, M. C. McCarthy, J. Sculley, J. Yu, H.-K. Jeong, H.-C. Zhou, *Coord. Chem. Rev.* **2011**, *255*, 1791.
[6] O. K. Farha, I. Eryazici, N. C. Jeong, B. G. Hauser, C. E. Wilmer, A. A. Sarjeant, R. Q. Snurr, S. B. T. Nguyen, A. Ö. Yazaydın, J. T. Hupp, *J. Am. Chem. Soc.* **2012**, *134*, 15016.
[7] H. Li, M. Eddaoudi, M. O'Keeffe, O. M. Yaghi, *Nature* **1999**, *402*, 276.
[8] H. K. Chae, D. Y. Siberio-Pérez, J. Kim, Y. B. Go, M. Eddaoudi, A. J. Matzger, M. O'Keefe, O. M. Yaghi, *Nature* **2004**, *427*, 523.
[9] M. Eddaoudi, J. Kim, N. Rosi, D. Vodak, J. Wachter, M. O'Keeffe, O. M. Yaghi, *Science* **2002**, *295*, 469.
[10] J.-R. Li, R. J. Kuppler, H.-C. Zhou, *Chem. Soc. Rev.* **2009**, *38*, 1477.
[11] N. L. Rosi, J. Eckert, M. Eddaoudi, D. T. Vodak, J. Kim, M. O'Keeffe, O. M. Yaghi, *Science* **2003**, *300*, 1127.
[12] D. L. Sarkisov, O. M. Yaghi, R. Q. Snurr, *Langmuir* **2004**, *20*, 2683.
[13] G. Férey, *Nature* **2005**, *436*, 187.
[14] R. Matsuda, R. Kitaura, S. Kitagawa, Y. Kubota, R. V. Belosludov, T. C. Kobayashi, H. Sakamoto, T. Chiba, M. Takata, Y. Kawazoe, Y. Mita, *Nature* **2005**, *436*, 238.
[15] L. J. Murray, M. Dincă, J. R. Long, *Chem. Soc. Rev.* **2009**, *38*, 1294.
[16] J. S. Seo, D. Whang, H. Lee, S. I. Jun, J. Oh, Y. J. Jeon, K. Kim, *Nature* **2000**, *404*, 982.
[17] D. Bradshaw, T. J. Prior, E. J. Cussen, J. B. Claridge, M. J. Rosseinsky, *J. Am. Chem. Soc.* **2004**, *126*, 6106.
[18] Z. R. Herm, E. D. Bloch, J. R. Long, *Chem. Mater.* **2013**, *26*, 323.
[19] J. Y. Lee, O. K. Farha, J. Roberts, K. A. Scheidt, S. B. T. Nguyen, J. T. Hupp, *Chem. Soc. Rev.* **2009**, *38*, 1450.
[20] J. Liu, L. Chen, H. Cui, J. Zhang, L. Zhang, C.-Y. Su, *Chem. Soc. Rev.* **2014**, *43*, 6011.
[21] M. Ranocchiari, J. A. van Bokhoven, *Phys. Chem. Chem. Phys.* **2011**, *13*, 6388.
[22] F. Luo, S. R. Batten, *Dalton Trans.* **2010**, *39*, 4485.
[23] I. Siepmann, Nanoporous Materials Genome Center, http://www.chem.umn.edu/nmgc/, accessed: January **2015**.
[24] Materials Innovation, Materials Genome Initiative, http://materialsinnovation.tms.org/genome.aspx, accessed: January **2015**.
[25] Y. J. Colón, R. Q. Snurr, *Chem. Soc. Rev.* **2014**, *43*, 5735.
[26] M. Fischer, J. R. B. Gomes, M. Jorge, *Mol. Simulat.* **2014**, *40*, 537.
[27] C. E. Wilmer, M. Leaf, C. Y. Lee, O. K. Fahra, B. G. Hauser, J. T. Hupp, R. Q. Snurr, *Nat. Chem.* **2012**, *4*, 83.
[28] Y. G. Chung, J. Camp, M. Haranczyk, B. J. Sikora, W. Bury, V. Krungleviciute, T. Yildirim, O. K. Farha, D. S. Sholl, R. Q. Snurr, *Chem. Mater.* **2014**, *26*, 6185.
[29] Y. Liu, H. Kabbour, C. M. Brown, D. A. Neumann, C. C. Ahn, *Langmuir* **2008**, *24*, 4772.
[30] E. D. Bloch, L. J. Murray, W. L. Queen, S. Chavan, S. N. Maximoff, J. P. Bigi, R. Krishna, V. K. Peterson, F. Grandjean, G. J. Long, B. Smit, S. Bordiga, C. M. Brown, J. R. Long, *J. Am. Chem. Soc.* **2011**, *133*, 14814.
[31] E. D. Bloch, W. L. Queen, R. Krishna, J. M. Zadrozny, C. M. Brown, J. R. Long, *Science* **2012**, *335*, 1606.
[32] S. Horike, M. Dincă, K. Tamaki, J. R. Long, *J. Am. Chem. Soc.* **2008**, *130*, 5854.

[33] Y.-S. Bae, C. Yeon Lee, K. C. Kim, O. K. Farha, P. Nickias, J. T. Hupp, S. B. T. Nguyen, R. Q. Snurr, *Angew. Chem. Int. Ed.* **2012**, *51*, 1857.
[34] T. M. McDonald, W. R. Lee, J. A. Mason, B. M. Wiers, C. S. Hong, J. R. Long, *J. Am. Chem. Soc.* **2012**, *134*, 7056.
[35] T. M. McDonald, J. A. Mason, X. Kong, E. D. Bloch, D. Gygi, A. Dani, V. Crocella, F. Giordanino, S. O. Odoh, W. Drisdell, B. Vlaisavljevich, A. L. Dzubak, R. Poloni, S. K. Schnell, N. Planas, K. Lee, T. Pascal, L. F. Wan, D. Prendergast, J. B. Neaton, B. Smit, J. B. Kortright, L. Gagliardi, S. Bordiga, J. A. Reimer, J. R. Long, *Nature* **2015**, *519*, 303.
[36] W. R. Lee, S. Y. Hwang, D. W. Ryu, K. S. Lim, S. S. Han, D. Moon, J. Choi, C. S. Hong, *Energy Environ. Sci.* **2014**, *7*, 744.
[37] N. L. Rosi, J. Kim, M. Eddaoudi, B. Chen, M. O'Keeffe, O. M. Yaghi, *J. Am. Chem. Soc.* **2005**, *127*, 1504.
[38] P. D. C. Dietzel, R. E. Johnsen, R. Blom, H. Fjellvåg, *Chem. Eur. J.* **2008**, *14*, 2389.
[39] P. D. C. Dietzel, R. Blom, H. Fjellvåg, *Eur. J. Inorg. Chem.* **2008**, *23*, 3624.
[40] S. R. Caskey, A. G. Wong-Foy, A. J. Matzger, *J. Am. Chem. Soc.* **2008**, *130*, 10870.
[41] W. Zhou, H. Wu, T. Yildirim, *J. Am. Chem. Soc.* **2008**, *130*, 15268.
[42] P. D. C. Dietzel, R. E. Johnsen, R. Blom, H. Fjellvåg, *Chem. Eur. J.* **2008**, *14*, 2389.
[43] P. D. C. Dietzel, R. Blom, H. Fjellvåg, *Eur. J. Inorg. Chem.* **2008**, *23*, 3624.
[44] S. Bhattacharjee, J.-S. Choi, S.-T. Yang, S. B. Choi, J. Kim, W.-S. Ahn, *J. Nanosci. Nanotechnol.* **2010**, *10*, 135.
[45] M. Dincă, A. Dailly, Y. Liu, C. M. Brown, D. A. Neumann, J. R. Long, *J. Am. Chem. Soc.* **2006**, *128*, 16876.
[46] M. Dincă, W. S. Han, Y. Liu, A. Dailly, C. M. Brown, J. R. Long, *Angew. Chem. Int. Ed.* **2007**, *46*, 1419.
[47] Biswas, M. Maes, A. Dhakshinamoorthy, M. Feyand, D. E. De Vos, H. Garcia, N. Stock, *J. Mater. Chem.* **2012**, *22*, 10200.
[48] K. Sumida, S. Horike, S. S. Kaye, Z. R. Herm, W. L. Queen, C. M. Brown, F. Grandjean, G. J. Long, A. Dailly, J. R. Long, *Chem. Sci.* **2010**, *1*, 184.
[49] S. S.-Y. Chui, S. M.-F. Lo, J. P. H. Charmant, A. G. Orpen, I. D. Williams, *Science.* **1999**, *283*, 1148.
[50] M. Kramer, U. Schwarz, S. Kaskel, *J. Mater. Chem.* **2006**, *16*, 2245.
[51] J. I. Feldblyum, M. Liu, D. W. Gidley, A. J. Matzger, *J. Am. Chem. Soc.* **2011**, *133*, 18257.
[52] L. J. Murray, M. Dincă, J. Yano, S. Chavan, S. Bordiga, C. M. Brown, J. R. Long, *J. Am. Chem. Soc.* **2010**, *132*, 7856.
[53] O. Kozachuk, K. Yusenko, H. Noei, Y. Wang, S. Walleck, T. Glaser, R. A. Fischer, *Chem. Commun.* **2011**, *47*, 8509.
[54] D. Yu, A. Ö. Yazaydin, J. R. Lane, P. D. C. Dietzel, R. Q. Snurr, *Chem. Sci.* **2013**, *4*, 3544.
[55] J. Borycz, L.-C. Lin, E. D. Bloch, J. Kim, A. L. Dzubak, R. Maurice, D. Semrouni, K. Lee, B. Smit, L. Gagliardi, *J. Phys. Chem C.* **2014**, *118*, 12230.
[56] L.-C. Lin, K. Lee, L. Gagliardi, J. B. Neaton, B. Smit, *J. Chem. Theory Comput.* **2014**, *10*, 1477.
[57] P. Canepa, C. A. Arter, E. M. Conwill, D. H. Johnson, B. A. Shoemaker, K. Z. Soliman, T. Thonhauser, *J. Mater. Chem.* **2013**, *1*, 13597.
[58] D. K. Britt, H. Furukawa, B. Wang, T. G. Glover, O. M. Yaghi, *Proc. Natl. Acad. Sci. USA* **2009**, *106*, 20637.
[59] A. Ö. Yazaydin, R. Q. Snurr, T.-H. Park, K. Koh, J. Liu, M. D. LeVan, A. I. Benin, P. Jakubczak, M. Lanuza, D. B. Galloway, J. J. Low, R. R. Willis, *J. Am. Chem. Soc.* **2009**, *131*, 18198.
[60] W. L. Queen, C. M. Brown, D. K. Britt, P. Zajdel, M. R. Hudson, O. M. Yaghi, *J. Phys. Chem. C.* **2011**, *115*, 24915.
[61] R. Poloni, B. Smit, J. B. Neaton, *J. Phys. Chem. A.* **2012**, *116*, 4957.
[62] Y. P Yao, N. Nijem, J. Li, Y. J. Chabal, D. C. Langreth, T. Thonhauser, *Phys. Rev. B* **2012**, *85*, 064302.
[63] L. Valenzano, B. Civalleri, S. Chavan, G. T. Palomino, C. O. Areán, S. Bordiga, *J. Phys. Chem. C* **2010**, *114*, 11185.
[64] H. Wu, J. M. Simmons, G. Srivivas, W. Zhou, T. Yildirim, *Chem. Lett.* **2010**, *1*, 1946.
[65] K. Lee, J. D. Howe, L.-C. Lin, B. Smit, J. B. Neaton, *Chem. Mater.* **2015**, *27*, 668.
[66] P. D. C. Dietzel, R. E. Johnsen, H. Fjellvåg, S. Bordiga, E. Groppo, S. Chavan, R. Blom, *Chem. Commun.* **2008**, 5125.
[67] X. Kong, E. Scott, W. Ding, J. A. Mason, J. R. Long, J. A. Reimer, *J. Am. Chem. Soc.* **2012**, *134*, 14341.
[68] L.-C. Lin, J. Kim, X. Kong, E. Scott, T. M. McDonald, J. R. Long, J. A. Reimer, B. Smit, *Angew. Chem. Int. Ed.* **2013**, *52*, 4410.
[69] W. L. Queen, M. R. Hudson, E. D. Bloch, J. A. Mason, M. I. Gonzalez, J. S. Lee, D. Gygi, J. D. Howe, K. Lee, T. A. Darwish, M. James, V. K. Peterson, S. J. Teat, B. Smit, J. B. Neaton, J. R. Long, C. M. Brown, *Chem. Sci.* **2014**, *5*, 4569.
[70] J. M. Huck, L.-C. Lin, A. Berger, M. N. Shahrak, R. L. Martin, A. Bhown, M. Haranczyk, K. Reuter, B. Smit, *Energy. Environ. Sci.* **2014**, *7*, 4136.
[71] G. Mills, H. Jónsson, G. K. Schenter, *Surf. Sci.* **1995**, *324*, 306.
[72] R. Poloni, K. Lee, R. F. Berger, B. Smit, J. B. Neaton, *Chem. Lett.* **2014**, *5*, 861.
[73] J. Park, H. Kim, S. S. Han, Y. Jung, *Chem. Lett.* **2012**, *3*, 826.
[74] K. Lee, W. C. Isley III, A. L. Dzubak, P. Verma, S. J. Stoneburner, L.-C. Lin, J. D. Howe, E. D. Bloch, D. A. Reed, M. R. Hudson, C. M. Brown, J. R. Long, J. B. Neaton, B. Smit, C. J. Cramer, D. G. Truhlar, L. Gagliardi, *J. Am. Chem. Soc.* **2014**, *136*, 698.
[75] A. L. Dzubak, L. C. Lin, J. Kim, J. A. Swisher, R. Poloni, S. N. Maximoff, L. Gagliardi, *Nat. Chem.* **2012**, *4*, 810.
[76] Y. He, R. Krishna, B. Chen, *Energy Environ. Sci.* **2012**, *5*, 9107.
[77] R. B. Eldridge, *Ind. Eng. Chem. Res.* **1993**, *32*, 2208.
[78] D.-L. Chen, H. Shang, W. Zhu, R. Krishna, *Chem. Eng. Sci.* **2014**, *117*, 407.
[79] S. Geier, J. A. Mason, E. D. Bloch, W. L. Queen, M. R. Hudson, C. M. Brown, J. R. Long, *Chem. Sci.* **2013**, *4*, 2054.
[80] P. Verma, X. Xu, D. G. Truhlar, *J. Phys. Chem. C* **2013**, *117*, 12648.
[81] H. Kim, J. Park, Y. Jung, *Phys. Chem. Chem. Phys.* **2013**, *15*, 19644.
[82] S. N. Maximoff, B. Smit, *Nat. Commun.* **2014**, *5*, 4032.
[83] K. Schlichte, T. Dratzke, S. Kaskel, *Micropor. Mesopor. Mater.* **2004**, *73*, 81.
[84] P. Horcajada, S. Surblé, C. Serre, D. Y. Hong, Y. K. Seo, J. S. Chang, J. M. Grenèche, I. Margiolaki, G Férey, *Chem. Commun.* **2007**, 2820.
[85] F. Vermoortele, M. Vandichel, B. Van de Voorde, R. Ameloot, M. Waroquier, V. Van Speybroeck, D. E. De Vos, *Angew. Chem. Int. Ed.* **2012**, *51*, 4887.
[86] J. Kim, S. Bhattacharjee, K.-E. Jeong, S.-Y. Jeong, W.-S. Ahn, *Chem. Commun.* **2009**, 3904.
[87] D. Ruano, M. Díaz-García, A. Alfayate, M. Sánchez-Sánchez, *ChemCatChem.* **2015**, *7*, 674.
[88] A. N. Mlinar, B. K. Keitz, D. Gygi, E. D. Bloch, J. R. Long, A. T. Bell, *ACS Catal.* **2014**, *4*, 717.
[89] J. Gascon, A. Corma, F. Kapteijn, F. X. Llabrés i Xamena, *ACS Catal.* **2014**, *4*, 361.
[90] A. Corma, H. García, F. X. Llabrés i Xamena, *Chem. Rev.* **2010**, *110*, 4606.
[91] *Metal Organic Frameworks as Heterogeneous Catalysts*, (Eds: F. Llabrés i Xamena, J. Gascon), Royal Society of Chemistry, Cambridge, UK **2013**.
[92] D. Farrusseng, S. Aguado, C. Pinel, *Angew. Chem. Int. Ed.* **2009**, *48*, 7502.
[93] J. Y. Lee, O. K. Farha, J. Roberts, K. A. Scheidt, S. T. Nguyen, J. T. Hupp, *Chem. Soc. Rev.* **2009**, *38*, 1450.

[94] D. J. Xiao, E. D. Bloch, J. A. Mason, W. L. Queen, M. R. Hudson, N. Planas, J. Borycz, A. L. Dzubak, P. Verma, K. Lee, F. Bonino, V. Crocellà, J. Yano, S. Bordiga, D. G. Truhlar, L. Gagliardi, C. M. Brown, J. R. Long, *Nat. Chem.* **2014**, *6*, 590.
[95] K. Tan, S. Zuluaga, Q. Gong, P. Canepa, H. Wang, J. Li, Y. J. Chabal, T. Thonhauser, *Chem. Mater.* **2014**, *26*, 6886.
[96] H. Li, C. E. Davis, T. L. Groy, D. G. Kelley, O. M. Yaghi, *J. Am. Chem. Soc.* **1998**, *120*, 2186.
[97] A. M. Shultz, O. K. Farha, J. T. Hupp, S. T. Nguyen, *J. Am. Chem. Soc.* **2009**, *131*, 4204.
[98] O. K. Farha, A. M. Shultz, A. A. Sarjeant, S. T. Nguyen, J. T. Hupp, *J. Am. Chem. Soc.* **2011**, *133*, 5652.
[99] D. Feng, Z.-Y. Gu, J.-R. Li, H.-L. Jiang, Z. Wei, H.-C. Zhou, *Angew. Chem. Int. Ed.* **2012**, *51*, 10307.
[100] D. Feng, K. Wang, Z. Wei, Y. P. Chen, C. M. Simon, R. K. Arvapally, R. L. Martin, M. Bosch, T.-F. Liu, S. Fordham, D. Yuan, M. A. Omary, M. Haranczyk, B. Smit, H.-C. Zhou, *Nat. Commun.* **2014**, *5*, 5723.
[101] U. Schubert, *Chem. Soc. Rev.* **2011**, *40*, 575.
[102] K. W. Chapman, G. J. Halder, P. J. Chupas, *J. Am. Chem. Soc.* **2008**, *130*, 10524.
[103] W. Sun, L. C. Lin, X. Peng, B. Smit, *AIChE J.* **2014**, *60*, 2314.
[104] S. Zuluaga, P. Canepa, K. Tan, Y. J. Chabal, T. Thonhauser, *J. Phys.: Condens. Matter.* **2014**, *26*, 133002.
[105] J. Vitillo, L. Regli, S. Chavan, G. Ricchiardi, G. Spoto, P. D. C. Dietzel, S. Bordiga, A. Zecchina, *J. Am Chem. Soc.* **2008**, *130*, 8386.
[106] W. L. Queen, E. D. Bloch, C. M. Brown, M. R. Hudson, J. A. Mason, A.-J. Cuesta-Ramirez, V. K. Peterson, J. R. Long, *Dalton Trans.* **2012**, *41*, 4180.
[107] W. S. Drisdell, R. Poloni, T. M. McDonald, J. R. Long, B. Smit, J. B. Neaton, D. Prendergast, J. B. Kortright, *J. Am. Chem. Soc.* **2013**, *135*, 18183.
[108] N. Rosenbach Jr., H. Jobic, A. Ghoufi, F. Salles, G. Maurin, S. Bourrelly, P. L. Llewellyn, T. Devic, C. Serre, G. Férey, *Angew. Chem. Int. Ed.* **2008**, *47*, 6611.
[109] L. Valenzano, J. G. Vitillo, S. Chavan, B. Civalleri, F. Bonino, S. Bordiga, C. Lamberti, *Catal. Today* **2012**, *182*, 67.
[110] H. C. Hoffmann, M. Debowski, P. Müller, S. Paasch, I. Senkovska, S. Kaskel, E. Brunner, *Materials* **2012**, *5*, 2537.
[111] A. Sutrisno, Y. Huang, *Solid State Nucl. Magn. Reson.* **2013**, *49–50*, 1.
[112] J. L. C. Rowsell, J. Eckert, O. M. Yaghi, *J. Am. Chem. Soc.* **2005**, *127*, 14904.
[113] S. Bordiga, E. Groppo, G. Agostini, J. A. van Bokhoven, C. Lamberti, *Chem. Rev.* **2013**, *113*, 1736.
[114] S. Chavan, O. Zavorotynska, C. Lamberti, S. Bordiga, *Dalton Trans.* **2013**, *42*, 12586.
[115] N. Nijem, J.-F. Veyan, L. Kong, K. Li, S. Pramanik, Y. Zhao, J. Li, D. Langreth, Y. J. Chabal, *J. Am. Chem. Soc.* **2010**, *132*, 1654.
[116] N. Nijem, J.-F. Veyan, L. Kong, H. Wu, Y. Zhao, J. Li, D. C. Langreth, Y. J. Chabal, *J. Am. Chem. Soc.* **2010**, *132*, 14834.
[117] R. L. Martin, M. Haranczyk, *Cryst. Growth Des.* **2014**, *14*, 2431.
[118] M. A. Addicoat, D. E. Coupry, T. Heine, *J. Phys. Chem. A* **2014**, *118*, 9607.
[119] S. Bureekaew, R. Schmid, *CrystEngComm.* **2013**, *15*, 1551.
[120] L. Valenzano, B. Civalleri, K. Sillar, J. Sauer, *J. Phys. Chem. C* **2011**, *115*, 21777.
[121] K. Sillar, J. Sauer, *J. Am. Chem. Soc.* **2012**, *134*, 18354.
[122] S. Grimme, *J. Comput. Chem.* **2006**, *27*, 1787.
[123] S. Grimme, S. Ehrlich, L. Goerigk, *J. Comput. Chem.* **2011**, *32*, 1456.
[124] M. Dion, H. Rydberg, E. Schröder, D. C. Langreth, B. I. Lundqvist, *Phys. Rev. Lett.* **2004**, *92*, 246401.
[125] K. Lee, E. D. Murray, L. Kong, B. I. Lundqvist, D. C. Langreth, *Phys. Rev. B.* **2010**, *82*, 081101.
[126] Y. Zhao, D. G. Truhlar, *Chem. Phys. Lett.* **2011**, *502*, 1.
[127] K. Berland, C. A. Arter, V. R. Cooper, K. Lee, B. I. Lundqvist, E. Schröder, P. Hyldgaard, *J. Chem. Phys.* **2014**, *140*, 18A539.
[128] S. L. Dudarev, G. A. Botton, S. Y. Savrasov, C. J. Humphreys, A. P. Sutton, *Phys. Rev. B* **1998**, *57*, 1505.
[129] R. Krishna, J. M. van Baten, *Sep. Purif. Technol.* **2012**, *87*, 120.
[130] J. M. Castillo, T. J. H. Vlugt, S. Calero, *J. Phys. Chem. C.* **2008**, *112*, 15934.
[131] M. Fischer, F. Hoffmann, M. Fröba, *ChemPhysChem.* **2010**, *11*, 2220.
[132] M. Fischer, B. Kuchta, L. Firlej, F. Hoffmann, M. Fröba, *J. Phys. Chem. C.* **2010**, *114*, 19116.
[133] L. Chen, L. Grajciar, P. Nachtigall, T. Düren, *J. Phys. Chem. C.* **2011**, *115*, 23074.
[134] L. Grajciar, A. D. Wiersum, P. L. Llewellyn, J.-S. Chang, P. Nachtigall, *J. Phys. Chem. C.* **2011**, *115*, 17925.
[135] M. Rubeš, L. Grajciar, O. Bludský, A. D. Wiersum, P. L. Llewellyn, P. Nachtigall, *ChemPhysChem.* **2012**, *13*, 488.
[136] L. Chen, C. A. Morrison, T. Düren, *J. Phys. Chem. C.* **2012**, *116*, 18899.
[137] Q. Yang, D. Liu, C. Zhong, J. R. Li, *Chem. Rev.* **2013**, *113*, 8261.
[138] T. F. Willems, C. H. Rycroft, M. Kazi, J. C. Meza, M. Haranczyk, *Microporous Mesoporous Mater.* **2012**, *149*, 134.
[139] R. L. Martin, B. Smit, M. Haranczyk, *J. Chem. Inf. Model.* **2012**, *52*, 308.
[140] M. Pinheiro, R. L. Martin, C. H. Rycroft, A. Jones, E. Iglesia, M. Haranczyk, *J. Mol. Graphics Modell.* **2013**, *44*, 208.
[141] S. L. Kinnings, N. Liu, P. J. Tonge, R. M. Jackson, L. Xie, P. E. Bourne, *J. Chem. Inf. Model.* **2011**, *51*, 408.
[142] R. L. Martin, C. M. Simon, B. Smit, M. Haranczyk, *J. Am. Chem. Soc.* **2014**, *136*, 5006.
[143] W. Lu, Z. Wei, Z.-Y. Gu, T.-F. Liu, J. Park, J. Park, J. Tian, M. Zhang, Q. Zhang, T. Gentle, M. Bosch, H.-C. Zhou, *Chem. Soc. Rev.* **2014**, *43*, 5561.